Dielectric Normal Mode Relaxation of Probe Polyisoprene Chain in Semidilute Polybutadiene Solutions. 1. End-to-End Distance

Osamu Urakawa, Keiichiro Adachi,* and Tadao Kotaka

Department of Macromolecular Science, Faculty of Science, Osaka University, Toyonaka, Osaka 560, Japan

Received November 3, 1992; Revised Manuscript Received January 14, 1993

ABSTRACT: Dielectric normal mode relaxation of a trace amount of *cis*-polyisoprene (PI) mixed in semidilute heptane (Hep) solutions of polybutadiene (PB) was studied and compared with semidilute PI/Hep solutions. The probe PI chains have the dipole moments aligned in the same direction parallel to the chain contour, but the matrix PB chains do not. Thus we can observe dynamic and conformational properties of the probe PI chains alone. In this part 1, the concentration dependence of the mean square end-to-end distance $\langle r^2 \rangle$ of PI was compared to those in PI/Hep and PI/PB/Hep solutions. In PI/Hep, the $\langle r^2 \rangle$ decreased with PI concentration C_I in proportion to $C^{-0.152}$. The exponent agreed well with the scaling theory of Daoud and Jannink with the Flory exponent $\nu = 0.56$. In PI/PB/Hep the C_I was fixed to be 0.2 or 0.4 wt % and the PB concentration C_B was changed over a wide range from dilute to semidilute regimes. In the case where the molecular weight M_I of PI is larger than that of PB (M_B), the $\langle r^2 \rangle$ of the PI chains divided by $\langle r^2 \rangle_0$ in dilute PI/Hep solution was plotted against $C_B[\eta]_B$ (with $[\eta]_B$ being the intrinsic viscosity of PB in Hep) and yielded a universal curve, whereas for those with $M_I \lesssim M_B$, a universal curve was obtained simply by plotting $\langle r^2 \rangle / M_I$ against C_B. The results were favorably compared with the scaling theories developed by Joanny et al. and Nose.

Introduction

In our previous papers, we reported dielectric normal mode relaxation of *cis*-polyisoprene (PI) in semidilute solutions of a good solvent benzene, moderately good solvents hexadecane and eicosene, and a Θ solvent dioxane.[1-3] Through such studies, we could determine, besides the dynamics of the global motions of the chains, the mean square end-to-end distance $\langle r^2 \rangle$ of the PI chains from the dielectric relaxation strnegth, although its applicability is limited only to Stockmayer's type-A polymers[4] that possess the dipole moment aligned in the same direction parallel to the chain contour. Conventional scattering techniques provide information only on the radii of gyration $\langle s^2 \rangle$,[5-7] although most of the theories deal with $\langle r^2 \rangle$ rather than $\langle s^2 \rangle$. Another advantage of the normal mode relaxation is that it reflects essentially the behavior of a single type-A chain regardless of its environment, either in solutions or in bulk or even in blends of other polymers. Unlike most other methods, the labeling of the sample is unnecessary in dielectric spectroscopy. For example, in determination of $\langle s^2 \rangle$ of a bulk polymer by small angle neutron scattering a small amount of the chains must be labeled with deuterium which might alter the thermodynamics of the system.

In the present study, we examined the behavior of a trace amount of PI chains dissolved in matrices of polybutadiene (PB)/heptane (Hep) semidilute solutions. A similar dielectric study of a ternary system has been made for the poly(ε-caprolactone)/poly(4-chlorostyrene)/dioxane system by Baysal and Stockmayer who are mainly interested in the dynamic properties.[8] In the PI/PB/Hep system, PB is not a type-A polymer and hence does not exhibit dielectric normal mode relaxation. Thus we can observe the $\langle r^2 \rangle$ (and dynamic properties as well) of the probe PI chains in such ternary solutions. For comparison, we also studied semidilute PI/Hep solutions. Here we report $\langle r^2 \rangle$ of the PI probe in a PI/PB/Hep ternary system as a function of the molecular weight M_I of PI itself, the molecular weight M_B of PB, and its concentration C_B in the matrix solutions. Especially two problems were examined: How the ratio of M_I/M_B and the interaction parameter between PI and PB affect the $\langle r^2 \rangle$ of PI as compared with those of a PI/Hep semidilute solution. The dynamic properties will be described in part 2 of this series.

Background of the Problems

Before describing the present problems, we briefly summarize their background. In a dilute solution of a flexible polymer of the degree of polymerization (DP) N, the chain expands by the excluded volume effect and the $\langle r^2 \rangle$ is proportional to $N^{2\nu}$ where ν is the Flory excluded volume exponent. In semidilute solution where polymer chains overlap each other, the excluded volume effect is partially screened and the N dependence of $\langle r^2 \rangle$ becomes weaker ($\langle r^2 \rangle \propto N$). With a further increase of polymer concentration the screening effect becomes intense and the dimension of the solute polymer decreases to the unperturbed value. The scaling theory[9,10] elegantly describes the concentration dependence of $\langle r^2 \rangle$ in the semidilute regime, considering the unit a so-called *blob* within which the excluded volume effect is exerted and without this the effect is screened, thus $\langle r^2 \rangle \propto g^{2\nu}(N/g) \propto NC^{(2\nu-1)/(1-3\nu)}$.

In ternary solutions especially consisting of a trace amount of a guest component (the N chain) whose DP = N dissolved in semidilute solutions of a matrix component (the P chain) with DP = P and a good solvent, the conformational features of the guest chains are classified into the following two categories. If N is much larger than P, the P chains behave as a solvent and the screening effect will hardly act on the N chain. On the other hand in the case of $N \leq P$, the normal screening effect equal to the case of $N = P$ is expected.

Flory[11] first treated this problem as the excluded volume effect of a single long N chain dissolved in a matrix of homologous short P chains (a binary blend) and concluded that the P chains behave as a good solvent, although the system is athermal, for the N chain and that the N chain is expanded when their DPs satisfy a certain condition, i.e., $N^{1/2} > P$. Joanny et al.[12,13] applied a scaling treatment and extended it to a ternary system composed of a single N chain, matrix P chains of the chemically same kind, and an athermal solvent. They reported that the Flory condition for the binary blend can be replaced by $(N/g_P)^{1/2}$

0024-9297/93/2226-2036$04.00/0

Table I
Characteristics of PI and PB

code	$10^{-3}M_w$	M_w/M_n	$[\eta]/g^{-1}$ cm^3	$10^2C^*/g$ cm^{-3}	methods
PI-86	86	1.06			GPC (Ca.)
PI-140	140	1.05	88.1	1.14	GPC (LS)
PI-651[a]	651	1.19			GPC (LS)
PI-222	222	1.07			LS
PI-542	542	1.06			LS
PI-743	743	1.07	249.6	0.401	LS
PI-1230	1230	1.07			LS
PB-13	13	1.05	20.9	4.78	GPC (LS)
PB-33	33	1.06	39.7	2.52	GPC (LS)
PB-63	63	1.04	64.8	1.54	GPC (LS)
PB-211	211	1.03	127.2	0.786	GPC (LS)
PB-521	521	1.15	224.5	0.445	GPC (LS)

[a] The data for this sample were not used in this part 1, but used in part 2.

$> P/g_P$, where g_P is the number of the monomeric units in the blob of the P chains. Replacing g_P by the relation $g_P \simeq C_P^{1/1-3\nu}$, they obtained $1 < C_P/C_P^* < (N/P)^{3\nu-1}$, where C_P is the matrix concentration and C_P^* ($\simeq P^{1-3\nu}$) is the *overlap* concentration of the P chain. In this concentration range the excluded volume effect between the blobs of the N chain is not fully screened and hence the N chain exhibits an anomalous behavior due to the interblob excluded volume effect. For example, $\langle r^2 \rangle$ is proportional to $N^{2\nu}$ (the excluded volume type) and differs with the P chains even in the solution of the same C_P. In a case of $N/P <$ 1, on the other hand, the $\langle r^2 \rangle$ of the N chain is equal to that of a semidilute solution in which $N = P$. Recently, Nose[14] extended the theory of Joanny et al. to a more general case in which the guest and matrix chains are chemically different. For the excluded volume problems in such ternary systems, however, few experiments[15-19] have been reported so far. A purpose of the present study is to provide a reliable experimental basis on which these theories can be tested.

Experimental Section

1. Materials. All PI and PB samples were prepared via anionic living polymerization in *n*-heptane at 20 ± 5 °C with *sec*-butyllithium. The weight average molecular weights M_w of four PI samples were determined by light scattering with a photogoniometer (Fica 50). For the other three PI and all PB samples, M_w were determined by using a gel permeation chromatograph (GPC) (Tosoh Model HLC-801A) equipped with a low-angle laser-light scattering detector (Tosoh Model LS-8000). The ratio of the weight to the number average molecular weight, M_w/M_n, was determined from the GPC diagram. The characteristics of the samples are summarized in Table I, in which the number in the sample code indicates the molecular weight in units of kilograms per mole.

The intrinsic viscosities $[\eta]$ were determined in heptane at 295 K. The results are given in Table I and cast into the Mark-Houwink-Sakurada equations.

$$[\eta]_B = 0.0521M_w^{0.638} \quad (1)$$

$$[\eta]_I = 0.0482M_w^{0.634} \quad (2)$$

Here and afterward the subscripts B and I represent PB and PI, respectively. The exponents indicate that heptane is a moderately good solvent for both PI and PB.

In ternary solutions the PI concentration C_I was fixed at ca. 2×10^{-3} g cm^{-3} for PI-743 and 4×10^{-3} g cm^{-3} for PI-140. The PB concentrations C_B were varied from 0 to 0.3 g cm^{-3}.

2. Measurements. Dielectric measurements were carried out with two transformer type capacitance bridges of General Radio 1615-A and Ando TR-IBK. The former covers the frequency (f) ranges of 100 Hz to 20 kHz, and the latter, 30 kHz to 1 MHz.

Figure 1 shows the cross-section of a newly designed capacitance cell used in this study. The cell was designed in such a way that liquid samples could be introduced into the cell from inlet D

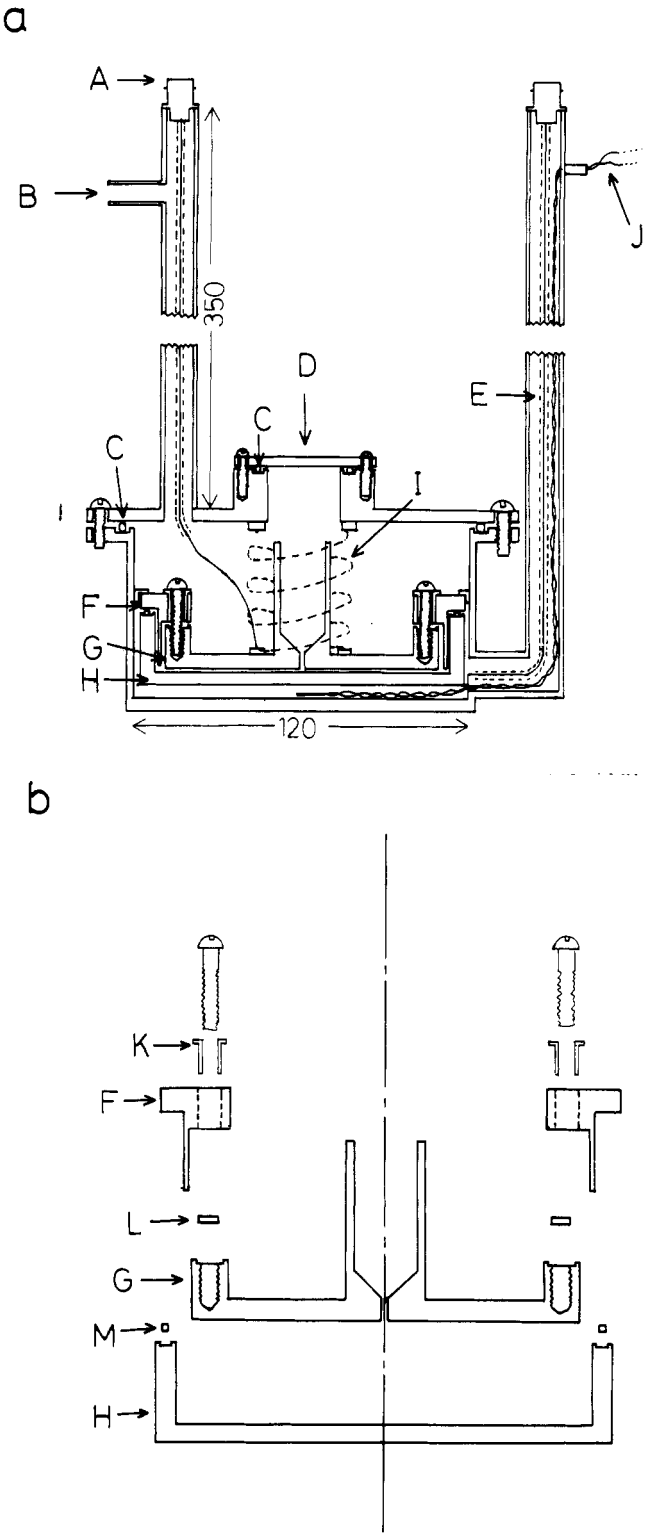

Figure 1. Cross-sectional view of the capacitance cell used in this study: (A) connector; (B) pipe for evacuation; (C) O-ring; (D) inlet of sample solutions; (E) lead wire; (F) guard; (G) guarded electrode; (H) unguarded electrode; (I) spring; (J) thermocouple; (K) Teflon insulator; (L) glass spacer; (M) glass spacer.

without dismantling the cell in order not to change the empty cell capacitance C_0 and to detect a weak signal from a trace amount of PI in dilute solutions. C_0 was ca. 130 pF, which was 5 times larger than conventional cells.

To minimize the error due to stray conductance, we first measured ϵ''_{solv} for pure solvent *n*-heptane. Then we replaced the solvent by a test solution without dismantling the cell and we measured the ϵ''_{soln} of the solution. The net ϵ'' of the solution was determined by subtracting ϵ''_{solv} from ϵ''_{soln}. This operation was necessary only for the measurement at the high f range from 30 kHz to 1 MHz. We expect that the error in ϵ'' thus determined was less than 10% at most and usually less than 2%.

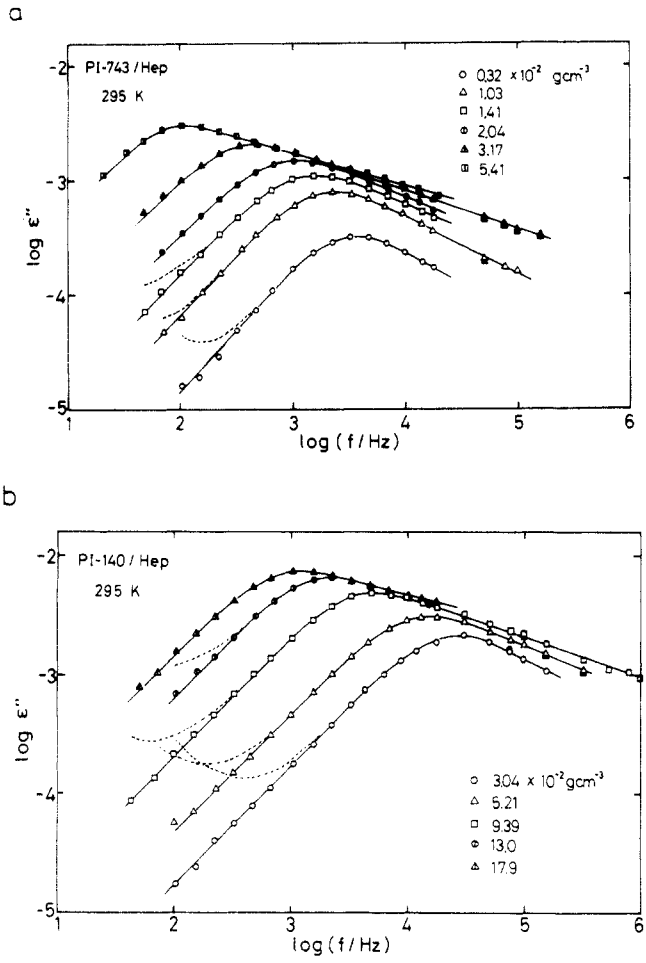

Figure 2. Representative loss curves for PI solutions in heptane at 295 K: (a) PI-743/heptane system; (b) PI-140/heptane system. Concentrations are given in the figure.

The relaxation strength $\Delta\epsilon$ was determined by the standard method of calculating the area under the ϵ'' curve by

$$\Delta\epsilon = (2/\pi)\int_{-\infty}^{\infty}\epsilon''\, d\ln f \tag{3}$$

When the frequency range of measurement was limited, we assumed that the $\Delta\epsilon$ is proportional to the maximum value ϵ''_{max} of the loss multiplied by the half-width δ i.e., $\Delta\epsilon \simeq K\epsilon''_{max}\delta$. The constant K was estimated to be 1.79 from the ϵ'' curves measured over a wide frequency range. Another method to estimate $\Delta\epsilon$ is the extrapolation of the ϵ'' curve using the Havriliak–Negami[20] equation. However in the present case the ϵ'' curves do not fit well to the equation in the low frequency side of the peak. Therefore we did not use this method. The error limit in the determination of $\Delta\epsilon$ is estimated to be within 15%.

3. Evaluation of the Mean Square End-to-End Distance. The relation between the dielectric relaxation strength $\Delta\epsilon$ and the mean square end-to-end distance $\langle r^2\rangle$ is given by

$$\frac{\Delta\epsilon}{C_I} = \frac{4\pi N_A \mu^2}{3k_B T}\frac{\langle r^2\rangle}{M_I}F \tag{4}$$

where μ is the dipole moment per unit contour length of PI and F is the ratio of the internal and external fields. Generally, F is a function of the dielectric constant of the medium. However, for the normal mode process, we proposed that F is close to unity since the local inhomogeneity of electric field is smeared out in the scale of the end-to-end distance of the polymer chains.[21] It is noted that in the present paper we deal with the relative change in $\langle r^2\rangle$, and thus, even if F is greater than unity, we expect that at least the relative value of $\langle r^2\rangle$ is meaningful.

Results and Discussion

1. Dielectric Loss Curves. Parts a and b of Figure 2 show representative dielectric loss factors ϵ'' for heptane solutions of PI-743 and PI-140. The dashed lines indicate raw data. The increase of ϵ'' in the low frequency range is due to ionic conduction since the dielectric constant ϵ' is independent of frequency in this frequency range. The contribution of the ionic conduction g_{dc} to ϵ'' was estimated by plotting alternating conductivity g against f^2 since at the end of the normal mode relaxation (low frequency side) ϵ'' is proportional to f and g is proportional to f^2. The value of g at $f = 0$ was estimated by linear extrapolation and was assumed to be the direct current conductivity.

It is seen that log ϵ'' vs log f at frequencies far from the loss maximum is almost straight. This behavior was also observed for concentrated solutions and bulk PI.[22,23] Similar behavior was also observed in PI/PB/Hep ternary systems. In the previous section we assumed that the area under the ϵ'' vs log f curve was proportional to the half-width δ and ϵ''_{max}. This assumption may be reasonable since the shape of the ϵ'' curve changes with concentration as the scale expansion at the high f side from f_{max}.

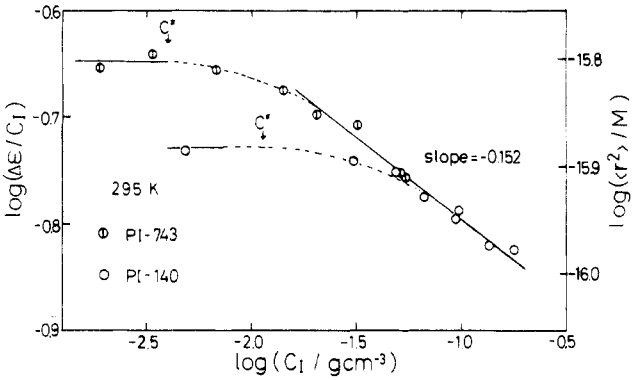

Figure 3. Double logarithmic plot of $\langle r^2\rangle/M$ vs PI concentration C_I at 295 K for PI/heptane binary solutions. The arrows indicate the overlap concentration determined as $1/[\eta]$.

2. Concentration Dependence of $\langle r^2\rangle$ in the PI/Heptane System. The mean square end-to-end distance $\langle r^2\rangle$ of the PI chains was determined by using eq 4. Figure 3 shows the concentration dependence of $\langle r^2\rangle$ for PI-743 and PI-140 solutions. When C is above C^*, $\langle r^2\rangle$ begins to decrease with C. Here the critical concentration C^*, where polymer coils begin to overlap, was evaluated by the relation $C^* \simeq 1/[\eta]$. This is due to the onset of screening of the excluded volume effect.

According to Daoud and Jannink,[10] the M and C dependence of $\langle r^2\rangle$ in semidilute regime is given by

$$\langle r^2\rangle \propto MC^{(2\nu-1)/(1-3\nu)} \tag{5}$$

where ν is the excluded volume exponent equal to $^3/_5$ in a good solvent and $^1/_2$ in a Θ solvent. From eq 5, we see that $\langle r^2\rangle/M$ becomes independent of M and proportional to $C^{(2\nu-1)/(1-3\nu)}$. As is seen in Figure 3 when C is larger than $5C^*$, the values of $\langle r^2\rangle/M$ for PI-743 and PI-140 coincide and conform to a straight line with the slope of 0.152 that corresponds to $\nu = 0.56$ in eq 5. We expect that the ratio of $\langle r^2\rangle$ at concentration C and the $\langle r^2\rangle_0$ which is the dimension expanded in the dilute solution is a universal function of C/C^*. Here C/C^* represents the extent of overlapping of coils, $C^* \propto M^{1-3\nu}$:

$$\langle r^2\rangle/\langle r^2\rangle_0 = 1 \qquad C < C^* \tag{6}$$

$$\langle r^2\rangle/\langle r^2\rangle_0 = (C/C^*)^{(2\nu-1)/(1-3\nu)} \qquad C > C^* \tag{7}$$

Figure 4 shows a double logarithmic plot of $\langle r^2\rangle/\langle r^2\rangle_0$ vs C/C^* for these solutions. In this concentration range all the data are successfully superposed and well represented by eqs 6 and 7 except for the crossover of dilute to semidilute regime.

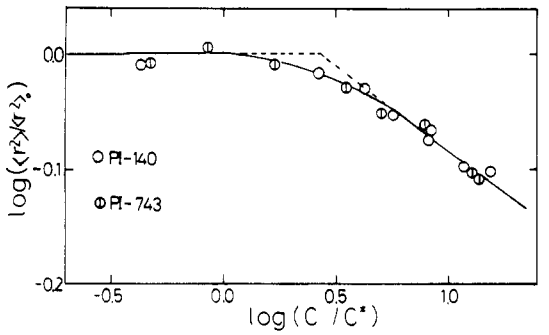

Figure 4. Reduced plot of $\langle r^2\rangle/\langle r^2\rangle_0$ vs C/C^*. Here $\langle r^2\rangle_0$ represents the dimension expanded in dilute solution. The dashed line is the theoretical prediction of eqs 6 and 7.

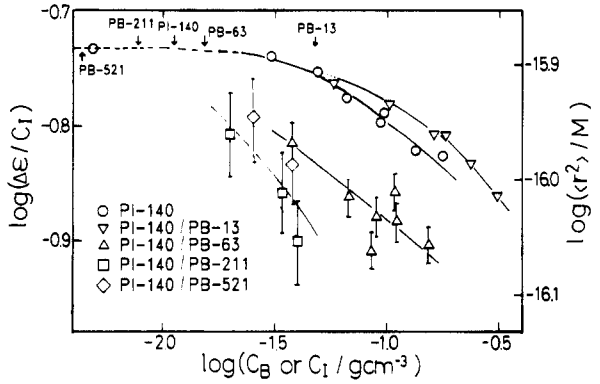

Figure 5. Double logarithmic plot of $\langle r^2\rangle/M$ of PI-140 vs PB concentration C_B. The data of PI/heptane binary solutions are also plotted against log C_I. The arrows indicate the C^* for each matrix solution. The large error bars in high M_w PB solutions are due to the lack of data of the half-width δ for ϵ'' curves because the peak is located at high frequency. The error in the PI/Hep (○) and PI-140/PB-13/Hep (▽) systems is similar to that of the PI-140/PB-63/Hep (△) system. The solid lines are guides for the eyes.

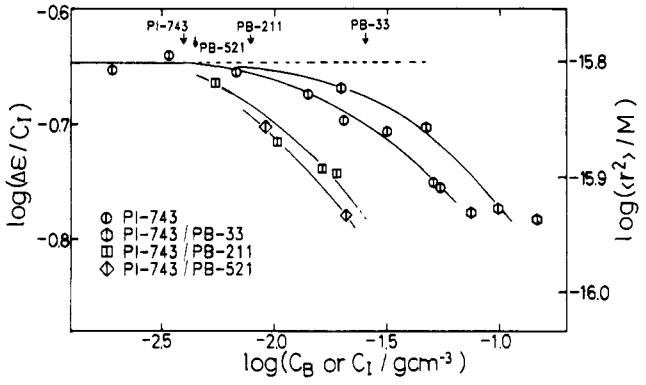

Figure 6. Double logarithmic plot of $\langle r^2\rangle/M$ of PI-743 vs C_B. The arrows indicate C^*. The solid lines are guides for the eyes.

3. PI/PB/Heptane Ternary Systems. Ternary solutions are different from binary solutions in the following two aspects: (1) the different molecular weight of surrounding PB chains (M_B) from the guest PI chain (M_I) and (2) the interaction between PI and PB. Taking into account these problems, we will describe the experimental results.

Figure 5 shows $\Delta\epsilon/C_I$ ($\propto\langle r^2\rangle/M$) for PI-140 plotted against the PB concentration C_B of PB-13, PB-63, PB-211, and PB-521. Figure 6 shows the similar plot for PI-743 in solutions of PB-33, PB-211, and PB-521. The data for PI/Hep binary solutions are also plotted against the PI concentration C_I. As mentioned in the Experimental Section, C_I was fixed to be 2×10^{-3} g cm^{-3} for the PI-743/PB/Hep system and 4×10^{-3} g cm^{-3} for PI-140/PB/Hep. These concentrations are less than the C^* of PI.

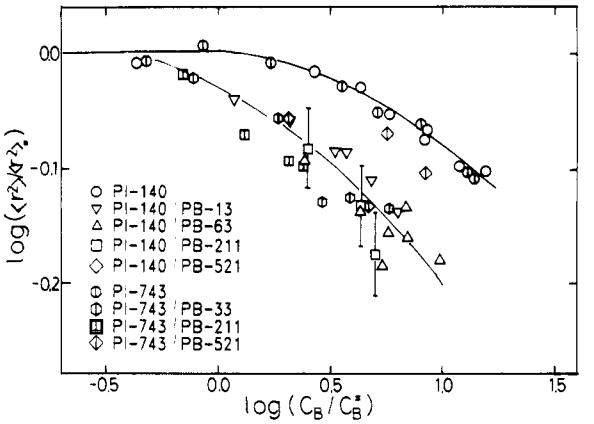

Figure 7. Reduced plot of $\langle r^2\rangle/\langle r^2\rangle_0$ vs C_B/C_B^* for PI/PB/Hep solutions. The solid lines indicate guides for the eyes.

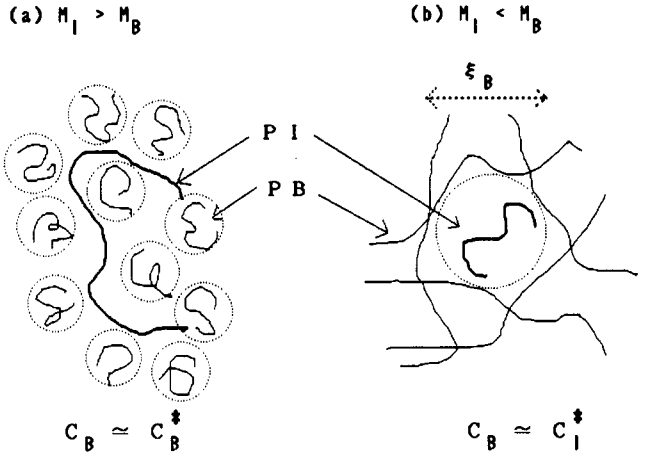

Figure 8. Schematic representation of a guest PI chain in semidilute PB solution. The PI chain begins to shrink at (a) $C_B \simeq C_B^*$ when $M_I > M_B$ and at (b) $C_B \simeq C_I^*$ when $M_I < M_B$. At condition (b), ξ_B is equal to the end-to-end distance of the PI chain.

Thus the PI chains do not overlapped each other though the PB chains are in semidilute regime.

Looking at the data of ternary systems, we see that the curves of $\langle r^2\rangle$ as a function of C_B are located at a lower $\langle r^2\rangle$ level with increasing M_B, but when M_B/M_I is larger than unity, the $\langle r^2\rangle$ of PI becomes independent of M_B (see data for PI-140/PB-521 in Figure 5). Thus we found the matrix molecular weight is very important for the guest chain dimension. For the case of $M_I/M_B > 1$, the concentration where $\langle r^2\rangle$ of PI begins to decrease is close to C_B^*. Thus we tried to reduce the data of Figures 5 and 6 by $\langle r^2\rangle_0$ and C_B^* in Figure 7. We can see that all curves approximately converge on one curve except for the PI-140/PB-521 system. This indicates that the quality of the PB matrix solution regarded as a "solvent" is determined by the parameter C_B/C_B^* for the case $M_I/M_B > 1$. In the opposite case ($M_I/M_B < 1$), since the $\langle r^2\rangle^{1/2}$ of PI is smaller than that of PB, the screening length ξ_B of the PB solution within whose distance the monomer distribution is of the excluded-volume type can be larger than $\langle r^2\rangle^{1/2}$ of PI. In such a case the screening effect does not act upon the PI chain. Thus PI expands as in a pure good solvent. But when ξ_B becomes nearly equal to the $\langle r^2\rangle^{1/2}$ of PI, the PI chain will begin to shrink by the screening effect. Figure 8 shows the schematic representation of the guest PI chain beginning to shrink in the cases of (a) $M_I/M_B > 1$ and (b) $M_I/M_B < 1$. In case a the shrinkage starts at $C_B \simeq C_B^*$, but in the opposite case (b) it starts at $C_B \simeq C_I^*$ where the $\langle r^2\rangle^{1/2}$ of PI is nearly equal to ξ_B. In case b the dimension of the PI chain does not depend on M_B but depends only on the mesh size (screening length)

which is proportional to $C_B^{\nu/1-3\nu}$, thus the curves of $\langle r^2\rangle$ vs C_B are considered to become universal as was seen in PI/Hep semidilute solutions (Figure 3). In Figure 9 we plotted $\Delta\epsilon/C_I$ against C_B for PI-140/PB-211, PI-140/PB-521, and PI-743/PB-521 solutions and for comparison we also plotted the data of PI/Hep solutions against C_I. We can see these data for ternary solutions are on one curve. Thus in the case of $M_I/M_B < 1$, $\langle r^2\rangle$ is independent of M_B and determined only by C_B.

Kuhn et al.[15,16] and Lin and Rosen[17] made light scattering studies for the dimension of a large polystyrene (PS) chain dissolved in an isorefractive poly(methyl methacrylate) (PMMA)/solvent system. They found that the second virial coefficient A_2 of PS decreased with C_{PMMA}. They also found that the Θ concentration (C_Θ) of C_{PMMA} at which $A_2 = 0$ was proportional to $1/[\eta]$ ($\propto C^*$) and that the C_{PMMA} dependence of radii of gyration $\langle s^2\rangle$ could be expressed by the universal form, $\langle s^2\rangle/\langle s^2\rangle_0 \simeq f(C/C_\Theta)$ in the case of $M_{PS} > M_{PMMA}$. Our result is consistent with theirs if we assume the proportionality of $C_B^* \propto C_\Theta$. The case of $M_{PS} < M_{PMMA}$ was minutely investigated by Numasawa et al.[18] who made similar measurements to Kuhn et al. They reported that at the matrix concentration where $\xi \simeq \langle s^2\rangle^{1/2}$, A_2 became zero but $\langle s^2\rangle$ of PS chain expanded as in the good solvent because the intrachain excluded volume effect was not screened out. In such a case C_Θ is not proportional to the C^* of the matrix solution and is independent of molecular weight of the matrix polymer. Thus the universality with C/C^* becomes invalid. In Figure 7 we can see $\langle r^2\rangle$ values for PI-140/PI-521 are higher than the $\langle r^2\rangle$ given by the universal curve as observed by Kuhn et al.

The second noteworthy difference between PI/PB/Hep and PI/Hep solutions is due to the interaction between PI and PB. In Figure 5, we see that $\langle r^2\rangle$ of PI-140 in the binary PI/Hep system is larger than that in the ternary systems except for the case where M_B is much lower than M_I. The same relation is also observed in solutions of PI-743, as shown in Figure 6. Thus the $\langle r^2\rangle$ of a PI chain in solutions of the same PI chains is larger than that in solutions of PB. If we regard the PI or PB solution surrounding a test chain as a "solvent", the quality of PI solution is better than PB solution at the same concentration: The interaction parameter between the PI and PB chains is positive. In Figures 7 and 9, the difference in $\langle r^2\rangle$ between PI/PB/Hep and PI/Hep is also due to the interaction between PI and PB chains.

Scaling Theory. Nose[14] calculated the dimension of a single test chain (N chain) with the degree of polymerization DP = N in a matrix consisting of chemically different P chains in an athermal solvent. The interaction parameter between N and P chains is χ. He discussed the behavior for the cases where (i) $N \gg P$ and (ii) $N \le P$.

To review the theory, we first summarize the simplest case of $\chi = 0$: N and P chains are chemically identical, and this is almost equivalent to the theory of Joanny et al.[12,13] In case i where $N \gg P$, the theory predicts that there are three regimes in which C_P dependence of $\langle r^2\rangle$ is different. In regime i-I, the matrix P chains do not overlap each other and hence $C_P/C_P^* < 1$ where C_P^* is the overlapping concentration. In this regime the dimension of the N chain is nearly equal to that in pure solvent:

$$\langle r^2\rangle \simeq a^2N^{2\nu} \tag{8}$$

where a is the length of the monomer unit. In regime i-II, the short P chain begins to overlap but C_P is not still very high, $1 < C_P/C_P^* < (N/P)^{3\nu-1}$:

$$\langle r^2\rangle \simeq a^2N^{2\nu}(C_P/C_P^*)^{2(2\nu-1)/(1-3\nu)} \tag{9}$$

In this regime, the excluded volume effect between blobs for the N chain is still prevailing and the absolute value of the exponent is 2 times larger than the polymer/solvent binary system (eq 5). And the reduced end-to-end distance $\langle r^2\rangle/\langle r^2\rangle_0$ can be expressed by the universal function of C_P/C_P^*. In regime i-III, $C_P/C_P^* > (N/P)^{3\nu-1}$:

$$\langle r^2\rangle \simeq a^2NC_P^{(1-2\nu)/(3\nu-1)} \tag{10}$$

In this regime the excluded volume effect between blobs is completely screened; thus the N dependence is of the Gaussian type and the exponent to C_P is equal to that of eq 5. This equation can be rewritten as in Table II. Thus it cannot be reduced by C_P^*.

In case ii where $N \le P$, two regimes appear: The regime where $C_P < C_N^*$ is referred to as regime ii-I where $\langle r^2\rangle^{1/2}$ of the N chain is smaller than the screening length ξ_P of the matrix solution thus the N chain expands as in the pure solvent. $\langle r^2\rangle$ is given by

$$\langle r^2\rangle \simeq a^2N^{2\nu} \tag{11}$$

When $C_P < C_N^*$, referred to as regime ii-II, $\langle r^2\rangle^{1/2} > \xi_P$. Thus the excluded volume effect is screened and $\langle r^2\rangle$ is given by

$$\langle r^2\rangle \simeq a^2NC_P^{(1-2\nu)/(3\nu-1)} \tag{12}$$

In these regimes (ii-I,II), $\langle r^2\rangle$ is completely independent of P and cannot be reduced by C_P^*. These theoretical classifications are summarized in Table II.

Table II
Theoretical Classification of Guest Chain Dimension

concn	$\langle r^2\rangle/\langle r^2\rangle_0$	regime
	(i) $N \gg P$	
$C_P/C_P^* < 1$	1	i-I
$1 < C_P/C_P^* < (N/P)^{3\nu-1}$	$(C_P/C_P^*)^{2(1-2\nu)/(3\nu-1)}$	i-II
$C_P/C_P^* > (N/P)^{3\nu-1}$	$(C_P/C_N^*)^{(1-2\nu)/(3\nu-1)}$	i-III
	(ii) $N < P$	
$C_P/C_N^* < 1$	1	ii-I
$C_P/C_N^* > 1$	$(C_P/C_N^*)^{(1-2\nu)/(3\nu-1)}$	ii-II

To take into account the interaction parameter χ between the N and P chains, the classification of nature for the dimension of the guest N chain is almost unchanged. But the difference is that the Θ concentration C_Θ where the two-body interaction between guest N chains changes from repulsive to attractive appears. When $C \gg C_\Theta$, the intrachain excluded volume effect in an N chain becomes attractive and the chain collapses;

$$\langle r^2\rangle \simeq a^2N^{2/3}C_P^{-2/3}\chi^{-2/3} \tag{13}$$

But at $C < C_\Theta$, the regions discussed above remain and especially in regimes i-I and -II the universality with C_P/C_P^* holds well in such a case of $\chi > 0$ but the dependence on C_P becomes slightly strong.

Comparison with Theory. As is seen in Figure 7, $\langle r^2\rangle/\langle r^2\rangle_0$ vs C_B/C_B^* converges on one curve in the case of $M_I > M_B$. The theory predicts that if $N \gg P$, the C dependence of $\langle r^2\rangle/\langle r^2\rangle_0$ is given by eqs 8 and 9 and hence the data for $\langle r^2\rangle/\langle r^2\rangle_0$ in solutions of PIs with various M_B fall on the universal curve of C_B/C_B^*. Thus our experimental results may be explained by considering that the present system is in regimes i-I (eq 8) and i-II (eq 9). However there are two disagreements with the theory. One is that the slope in Figure 7 is expected to be 2 times larger than that in PI/Hep binary systems (eqs 8 and 9). Actually, we see that the slope is almost the same between binary and

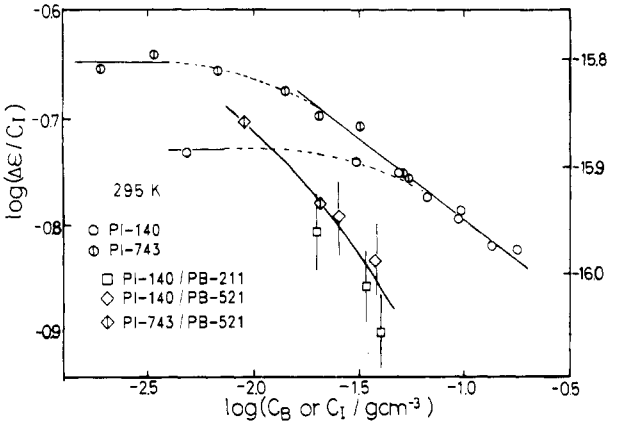

Figure 9. Double logarithmic plot of $\langle r^2\rangle/M$ of PI for PI-743/PB-521, PI-140/PB-211, and PI-140/PB-521 solutions. The data for PI/Hep solutions are also plotted in this figure. The dashed line indicates the crossover region.

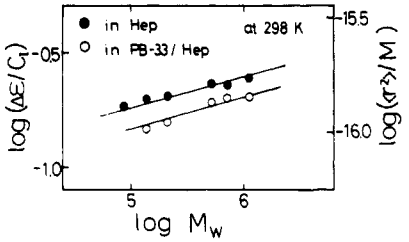

Figure 10. Dependence of $\langle r^2\rangle/M$ on the molecular weight of PI in heptane dilute solution and PB-33/Hep semidilute solution ($C_B = 4.84 \times 10^{-2}$ g cm^{-3}).

ternary systems. This may be explained as follows. Since our experiment did not cover the wide range of C_B, the observed slope has not reached the asymptotic value. The second disagreement is that the theory predicts that regime i-II appears only when $N \gg P$, e.g., $N/P > 10$. But, as seen in Figure 7, the data for $M_I/M_B < 10$ converge. This result is not explained by the theory.

In Figure 9, three curves of $\langle r^2\rangle$ for PI-140/PB-211, PI-140/PB-521, and PI-743/PB-521 approximately coincide within the experimental error. This behavior may be explained by assuming that these solutions are in case ii.

We conclude that the theory explains roughly the experimental result, but does not do so quantitatively.

4. M_I Dependence of $\langle r^2\rangle$. In the previous section, we discussed the C_B dependence of $\langle r^2\rangle$. We discuss here the M_I dependence of $\langle r^2\rangle$ for dilute PI in a PB matrix solution in which $C_B = 4.84 \times 10^{-2}$ g cm^{-3} and $M_B = 3.3 \times 10^4$. Figure 10 shows the comparison of $\langle r^2\rangle/M$ for dilute PI in *n*-heptane and that in the PB/heptane semidilute solution. We see that the slopes are almost the same. This indicates that the excluded volume effect for the PI chain is not screened out even in the semidilute matrix solution. Such a phenomenon was predicted by the theory mentioned above. In the preceding section, we described that the excluded volume effect between blobs still prevails in regime i-II but that the absolute value of $\langle r^2\rangle$ is smaller than $\langle r^2\rangle_0$ by the factor of $(C_P/C_P^*)^{2(2\nu-1)/(1-3\nu)}$ (eq 9). The prediction agrees with this experimental result.

Conclusion

1. The mean square end-to-end distance $\langle r^2\rangle$ of the PI chain in PB semidilute solutions changes by PB concentration C_B and PB molecular weight M_B: $\langle r^2\rangle$ decreases with increasing C_B at fixed M_B. In the case where $M_I/M_B > 1$, $\langle r^2\rangle$ decreases with increasing M_B at fixed C_B and $\langle r^2\rangle/\langle r^2\rangle_0$ is approximately expressed by a universal function of C_B/C_B^*. In the case where $M_I/M_B < 1$, $\langle r^2\rangle$ is independent of M_B.

2. In semidilute solutions of low molecular weight PB, the excluded volume effect over the long range is not screened, as predicted by the theories of Nose and Joanny et al.

3. $\langle r^2\rangle$ of a PI chain in solutions of the same PI chains is larger than that in solutions of PB. This is due to the interaction between PI and PB.

Acknowledgment. This work was supported partly by the Institute of Polymer Research, Osaka University.

References and Notes

(1) Adachi, K.; Okazaki, H.; Kotaka, T. *Macromolecules* **1985**, *18*, 1687.
(2) Adachi, K.; Kotaka, T. *Macromolecules* **1988**, *21*, 157.
(3) Adachi, K.; Imanishi, Y.; Shinkado, T.; Kotaka, T. *Macromolecules* **1989**, *22*, 2391.
(4) Stockmayer, W. H. *Pure Appl. Chem.* **1967**, *15*, 539.
(5) Richards, R. W.; Macconachie, A.; Allen, G. *Polymer* **1978**, *19*, 266; **1981**, *22*, 147–157.
(6) King, J. S.; Boyer, W.; Wignall, G. D.; Ullman, R. *Macromolecules* **1985**, *18*, 709.
(7) Daoud, M.; Cotton, J. P.; Farnoux, B.; Jannink, G.; Sarma, G.; Benoit, H.; Duplessix, R.; Picot, C.; de Gennes, P. G. *Macromolecules* **1975**, *8*, 804.
(8) Baysal, B. M.; Stockmayer, W. H. *J. Mol. Liq.*, in press.
(9) De Gennes, P. G. *Scaling Concept in Polymer Physics*; Cornell University Press: Ithaca, NY, 1979.
(10) Daoud, M.; Jannink, G. *J. Phys. (Paris)* **1976**, *37*, 973.
(11) Flory, P. J. *J. Chem. Phys.* **1949**, *17*, 3, 303.
(12) Joanny, J. F.; Grant, P.; Turkerich, L. A.; Pincus, P. *J. Phys. (Paris)* **1981**, *42*, 1045.
(13) Joanny, J. F.; Grant, P.; Pincus, P.; Turkerich, L. A. *J. Appl. Phys.* **1981**, *52*, 5943.
(14) Nose, T. *J. Phys. (Paris)* **1986**, *47*, 517.
(15) Kuhn, R.; Cantow, H. J.; Burchard, W. *Angew. Makromol. Chem.* **1968**, *2*, 146.
(16) Kuhn, R.; Cantow, H. J. *Makromol. Chem.* **1969**, *122*, 65.
(17) Lin, C. Y.; Rosen, S. L. *J. Polym. Sci., Polym. Phys. Ed.* **1982**, *20*, 1497.
(18) Numasawa, N.; Hamada, T.; Nose, T. *J. Polym. Sci., Polym. Lett. Ed.* **1985**, *23*, 1.
(19) Cotts, D. B. *J. Polym. Sci., Polym. Phys. Ed.* **1983**, *21*, 13, 81.
(20) Havriliak, S.; Negami, S. *J. Polym. Sci., Part C* **1966**, No. 14, 99.
(21) Adachi, K.; Okazaki, H.; Kotaka, T. *Macromolecules* **1985**, *18*, 1486.
(22) Imanishi, Y.; Adachi, K.; Kotaka, T. *J. Chem. Phys.* **1988**, *89*, 7585.
(23) Adachi, K.; Imanishi, Y.; Kotaka, T. *J. Chem. Soc., Faraday Trans. 1* **1989**, *85*, 1083.